

Hopping ionic conductivity in Ce-doped SrF₂. I. Ionic thermocurrent results

P. Dorenbos, S. Vrind, J. Dolfig, and H. W. den Hartog

Solid State Physics Laboratory, University of Groningen, 1 Melkweg, 9718 EP Groningen, The Netherlands

(Received 31 July 1986)

In this paper we present ionic thermocurrent (ITC) results obtained for Sr_{1-x}Ce_xF_{2+x} single crystals (0.0001 < x < 0.4). From the dipolar relaxation peak in the ITC recordings the concentration of Ce³⁺-F⁻ dipolar complexes has been determined. We conclude that only isolated dipoles contribute significantly to the dipolar relaxation peak and that the dipoles are randomly distributed over the SrF₂ lattice. We find that in the dilutely doped crystals (x < 0.005) interstitial F⁻ ions dissociated from Ce³⁺-F⁻ dipolar complexes are responsible for an Arrhenius-type ionic conductivity. The position of the so-called high-temperature peak, observed in the ITC recordings, is directly proportional to the activation energy, from which the association energy of R³⁺-F⁻ dipolar complexes has been obtained (R = La, Ce, Pr, Nd, Eu, Sm, Gd, Er, Dy, Yb, Lu, or Y in SrF₂ or La, Eu, Gd, or Yb in BaF₂). At higher doping concentrations non-Arrhenius-type ionic conductivity, caused by hopping of interstitial F⁻ ions in the random potential energy barrier structure of the heavily doped fluorite lattice, is observed. In addition, results obtained from quenching experiments performed on Sr_{1-x}La_xF_{2+x} are presented.

I. INTRODUCTION

Single crystals with the fluorite structure (e.g., CaF₂, SrF₂, and BaF₂) doped with trivalent cation impurities (R³⁺) have been the subject of a lot of experimental and theoretical work. Concentrations of up to 50 mol % of the trivalent cations, which enter the crystal substitutionally, can be accommodated in the crystals without a change of the overall fluorite structure. An extra F⁻ ion, necessary for charge compensation, occupies an interstitial position preferably in the neighborhood of an R³⁺ ion, forming a dipolar complex. This interstitial ion can jump relatively easily from one interstitial site to an adjacent interstitial site, which may lead to polarization effects or ionic conductivity if an electric field is applied across the crystal.

In a recent paper¹ we have presented results obtained for SrF₂ doped with different rare-earth ions (La, Ce, Nd, Sm, Eu, Gd, Dy, Er, Yb, Lu). We have paid special attention to the concentration of NN and NNN dipolar complexes. These complexes consist of an R³⁺ ion and an interstitial F⁻ ion at a nearest-neighbor (NN) or a next-nearest-neighbor (NNN) site of the R³⁺. The number of dipolar defects has been determined by means of ionic thermocurrent (ITC) experiments. We concluded that as the radius of the R³⁺ ions decreases the probability of R³⁺ clustering increases, leading to extensive clustering in SrF₂ doped with the smaller ions (Dy, Er, Yb, Lu). Clustering is rather unimportant for the larger rare-earth ions (La, Ce, Pr, Nd), which is in line with experimental results obtained by Andeen *et al.*² and theoretical calculations performed by Corish *et al.*³ and Bendall *et al.*⁴

In the present paper we investigate the system Sr_{1-x}Ce_xF_{2+x} more extensively because of the absence of preferential clustering. In this system it is assumed that the defect structure can be described by a random distribution of Ce ions (and associated interstitial F⁻ ions) over

the available positions. We will first discuss the peaks observed in ITC recordings, which are associated with relaxations of bound charges. From the intensities of the peaks conclusions regarding the defect structure can be drawn. One of the relaxation peaks in the ITS recordings, the high-temperature (HT) peak, has been attributed¹ to the relaxation of F⁻ ions accumulated at the crystal surfaces during the polarization phase of the ITC experiment. Although we think that we have given convincing arguments¹ in support of the identification of this peak, recently our view has been questioned by Laredo *et al.*⁵ In the present paper we will give further evidence in support of our interpretation.

In the accompanying paper,⁶ which contains the second part of the investigation of Sr_{1-x}Ce_xF_{2+x}, results obtained with impedance measurements (at frequencies between 100–30 000 Hz and temperatures between 77 and 550 K) will be presented. Reference 6 will be devoted mainly to the ionic conductivity (σ) and the dielectric constant (ε) of intermediately doped materials (0.005 < x < 0.10), whereas in the current paper the defect structure and the ionic conductivity of dilutely doped crystals (x < 0.005) forms the main part.

II. THEORY AND EXPERIMENTAL PROCEDURES

The procedures for the growth of the crystals have been described elsewhere.⁷ After growing at ≅ 1750 K the crystals were cooled at a rate of ≅ 1 K/min to room temperature. We are dealing, therefore, with more or less annealed crystals. In the ITC and the dielectric experiments cylindrically shaped crystals, 7–8 mm in diameter and 1–2 mm thick, have been used. The Ce concentrations reported in this paper are the nominal concentrations. A detailed description of the ITC experiments and the interpretation of the ITC recordings has been given in Ref. 1.

In Fig. 1 a typical ITC recording obtained for SrF₂

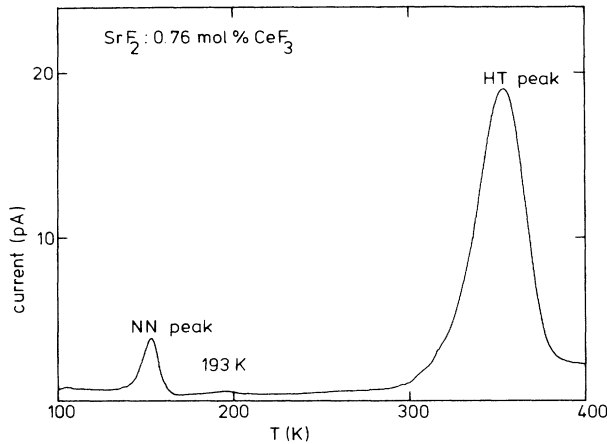


FIG. 1. Ionic thermocurrent recording of 0.76-mol % CeF_3 -doped SrF_2 .

doped with 0.76mol % Ce can be seen. The peak located around 152 K is due to polarization of $\text{Ce}^{3+}\text{-F}^-$ NN dipolar complexes. From the integrated intensity of this peak the capacitance increase of the crystals, caused by the NN dipole orientations, can be calculated. This capacitance (C_d) is related with the concentration of NN dipoles (N_d)

$$C_d = \frac{N_d \mu^2 A}{3k_B T_d}, \quad (1)$$

where μ is the dipole moment of a $\text{Ce}^{3+}\text{-F}^-$ NN dipolar complex, A is the area of the crystal, d is the crystal thickness, k_B is Boltzmann's constant, and T is the temperature (in K). Given μ , N_d can now be calculated. The position of the NN relaxation peak can be expressed by⁸

$$\frac{bE}{k_B T_m^2} \tau = 1, \quad (2)$$

where b is the linear heating rate used during the ITC recording (0.05 K/sec), T_m is the position of the NN relaxation peak (152 K), and τ is the relaxation time of a $\text{Ce}^{3+}\text{-F}^-$ dipolar complex. This relaxation time is thermally activated and can be written as

$$\tau = \tau_0 \exp \left[\frac{E}{k_B T} \right], \quad (3)$$

where E is the activation energy for the dipole relaxation. Values for τ_0 between 10^{-12} and 10^{-14} s and $E \cong 0.46$ eV have been reported.^{7,9}

The peak located at high temperatures (HT peak) has been attributed by us to a relaxation of F^- ions, accumulated at the crystal surfaces during polarization of the crystal, caused by the bulk ionic conductivity. The ionic thermocurrent as a function of the temperature [$I(T)$] can then be written as⁸

$$I(T) = (1-f)A \frac{fP_0}{\epsilon_0 \epsilon_s} \sigma(T) \exp \left[- \int_0^T \frac{\sigma(T')f}{b \epsilon_0 \epsilon_s} dT' \right], \quad (4)$$

where f is defined as $C_s/(C_I + C_s)$ and depends upon the geometry of the ITC-sample cell. C_s is the total capacitance of the crystal and C_I is the interfacial capacitance between the crystal surfaces and the electrodes. In the ITC experiments 0.1-mm Teflon® layers have been inserted between the crystal surfaces and the electrodes. The interfacial capacitance C_I is then equal to the capacitance of these Teflon® layers. P_0 is the total charge accumulated at the crystal surface; in case of total polarization of the crystal, P_0 is equal to $U_p C_I/A$, where U_p is the polarizing voltage (4 kV). ϵ_s is the static dielectric constant of the crystal and must be constant with the temperature in order for equation (4) to hold. ϵ_0 is the permittivity of vacuum and $\sigma(T)$ is the ionic conductivity at temperature T . From this equation it follows that the integrated intensity of the HT peak is completely determined by the initial polarization P_0 and by the ITC sample-cell configuration; it does not depend upon the ionic conductivity. The position, however, strongly depends upon the ionic conductivity. This has been expressed by the following condition, relating the position of the maximum current of the HT peak with the ionic conductivity,

$$\frac{d \ln[\sigma(T)]}{dT} = \frac{\sigma(T)f}{b \epsilon_0 \epsilon_s}. \quad (5)$$

When we define

$$Q(T) = \int_{t(T)}^{\infty} I(t') dt',$$

where the integration of the ionic thermocurrent is performed over the time; together with (4) we get⁸

$$\sigma(T) = \frac{I(T)}{Q(T)} \frac{\epsilon_0 \epsilon_s}{f}. \quad (6)$$

Equation (6) can be used for the calculation of the ionic conductivity from the HT peak.

III. EXPERIMENTAL RESULTS AND DISCUSSION

ITC experiments have been performed on $\text{Sr}_{1-x}\text{Ce}_x\text{F}_{2+x}$, where x ranges between 0.0001 and 0.35. In Fig. 2 the position of the HT peak (T_m) along with the width at half height (ΔT) have been plotted. Between $x = 0.0001$ and 0.005 the peak shifts slowly towards lower temperatures as the concentration of Ce impurities increases. The width of the peak remains almost constant (22 K). At higher concentrations the HT peak shifts rapidly towards lower temperatures and the width of the peak increases to approximately 40 K. At concentrations well above 10 mol % ($x = 0.1$) the peak stops shifting and the width decreases to 17 K. These features are very similar to the behavior of the HT peak of SrF_2 doped with La, Pr, and Nd.¹⁰⁻¹³ Many of the conclusions obtained in this paper pertain, therefore, also to SrF_2 doped with these impurities and vice versa.

A. The dipole relaxation peak

From the intensity of the NN dipole relaxation peak, located at 152 K (see Fig. 1), the concentration of $\text{Ce}^{3+}\text{-F}^-$ dipoles has been calculated with Eq. (1). We have

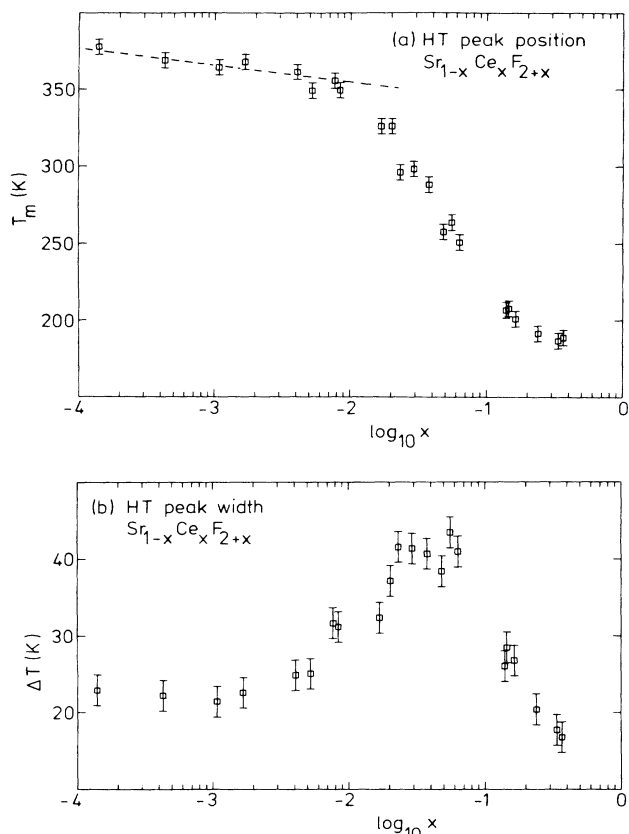


FIG. 2. (a) the position and (b) the width of the HT peak of $\text{Sr}_{1-x}\text{Ce}_x\text{F}_{2+x}$ as a function of the Ce concentration. The dashed line in (a) has a slope of -10 K/decades.

used for μ a value of 3.4×10^{-29} C m.¹⁴ The results have been plotted in Fig. 3 along with the results obtained from impedance measurements performed at a frequency of 300 Hz.⁶ The ITC and impedance data agree within the measuring accuracy. The experimental data points have been fitted with the following equation:

$$N_d = \frac{1}{2(d_{\text{F}^-})^3} \alpha x (1-x)^N \text{ dipoles/m}^3, \quad (7)$$

which is based on the assumption that only isolated dipoles contribute to the NN relaxation peak.¹ N represents the number of Sr^{2+} sites surrounding a dipole which may not be occupied by another defect (Ce^{3+} , $\text{Ce}^{3+}\text{-F}^-$ dipole, or another complex) for the dipole to be isolated. If the dipoles are distributed randomly, $x(1-x)^N$ represents the probability for this to occur. α is the fraction of Ce ions involved in a dipolar complex. d_{F^-} is the distance between lattice F^- ions in SrF_2 (2.90 Å). We have given in Ref. 15 a physical explanation for the assumption that only isolated dipoles contribute to the NN relaxation peak. It has been shown in Ref. 15 that changes in the association energy of F^- ions to a Ce ion of only 0.02–0.05 eV produce a drastic decrease of the orientational polarization. If an F^- ion located at one particular NN site surrounding a Ce ion has a somewhat larger association energy ($\cong 0.05$ eV) to the Ce ion than if the F^- ion is located at

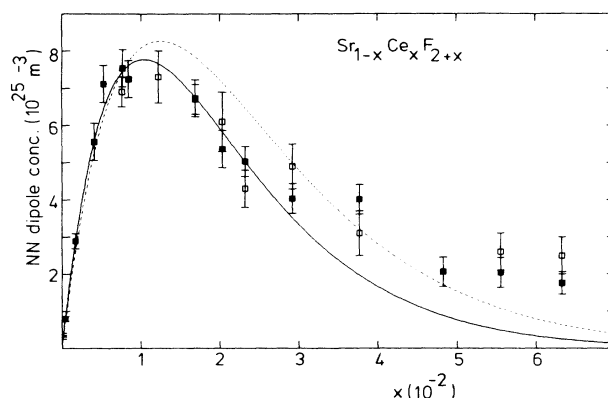


FIG. 3. Concentration of $\text{Ce}^{3+}\text{-F}^-$ NN-dipolar complexes in CeF_3 -doped SrF_2 . ■, data points obtained from ITC experiments. □, data points obtained from impedance measurements performed at a frequency of 300 Hz. The dashed curve represents the fitted dipole concentration with Eq. (7). The solid curve is obtained if only the data points up to 3 mol % are fitted.

one of the five other NN sites, the F^- ion will be pinned more or less at the former NN site. This pinning at the deepest site is responsible for a decrease in orientational polarization.

If the data points in Fig. 3 are fitted with Eq. (7) we obtain $\alpha = 0.83 \pm 0.05$ and $N = 79 \pm 5$; these results agree with previously published results.¹ The fit is, however, not very good. A possible explanation may be that the assumptions leading to Eq. (7) do not hold at high Ce concentrations because then the average distance between dipoles is rather small, and this may result in a deviation from a purely random distribution of the dipoles. Another explanation is that also nonisolated dipoles give a small contribution to the dipole relaxation peak. If only the data points up to a Ce concentration of 3 mol % are fitted we obtain $\alpha = 0.98 \pm 0.03$ and $N = 95 \pm 3$. α is now very close to unity implying that almost every Ce ion is involved in a $\text{Ce}^{3+}\text{-F}^-$ dipole complex and preferential clustering of the Ce ions does not take place at an extensive scale. From the value of N we conclude that $\cong 95$ Sr sites surrounding a dipolar complex should not be occupied by another defect in order for the dipole to be isolated. This corresponds with a sphere, centered around the Ce ion, with a radius of 10 Å.

In order to explain the decrease of the dipole concentration for Ce concentrations higher than 1 mol % the influence of a defect located at a distance of 10 Å from a central dipole on the reorientational kinetics should be considered. Due to Coulombic and elastic interactions between the defects the potential energies and barriers change from NN site to NN site. If we neglect the elastic interactions and assume that the electrostatic interactions can be described by a screened Coulomb potential Eq. (8), the potential energies and barrier heights for the NN sites and the saddle points between the NN sites can be calculated:

$$V = \frac{1}{4\pi\epsilon_0} \frac{q}{\epsilon_s R}, \quad (8)$$

where q is the elementary charge, R is the distance and ϵ_s is the static dielectric constant of SrF_2 [6.47 (Ref. 16)]. Depending upon the orientation of the disturbing dipole with respect to the central dipole we calculate with (8) changes in the binding energies of $\text{Ce}^{3+}\text{-F}^-$ dipoles up to 0.06 eV. The same changes have also been calculated for the potential energy barriers between NN sites. With these energy changes a reduction of the orientational polarization of the central dipole with a factor 10–20 is expected,¹⁵ which gives a plausible explanation for the assumption that only isolated dipoles contribute significantly to the dipole relaxation peak.

B. The 193 K relaxation peak

Andeen *et al.*² have presented dielectric loss results obtained for SrF_2 doped with rare-earth ions. Next to NN dipole and NNN dipole relaxation peaks a third peak shifting towards lower temperatures as the ionic radius of the rare-earth ion decreases was observed. This peak, located at a temperature around 193 K in Fig. 1, has been attributed to relaxations of F^- ions bound to a cluster of rare-earth ions. Quenching experiments performed by Figueroa *et al.*¹⁷ on SrF_2 doped with La showed that the intensity of this peak decreases, accompanied by an increased NN peak intensity. Due to the high quenching temperatures the clusters dissociate and NN complexes are formed. den Hartog *et al.*¹² have held NNN relaxations responsible for the 193 K peak. This was based on combined ITC and loss experiments. The answer to the question of the true origin of the 193 K peak will be left open in this paper. It will, however, not be essential for the discussion of the observed ionic conductivity, in which we are mainly interested.

C. Quenching experiments performed on $\text{Sr}_{1-x}\text{La}_x\text{F}_{2+x}$

In order to study the change of the defect structure upon quenching of the crystals we have performed ITC measurements on quenched crystals of $\text{Sr}_{1-x}\text{La}_x\text{F}_{2+x}$ ($x=0.001, 0.005, 0.015, \text{ and } 0.033$). First the crystals were annealed at 1300 K for 16 h and quenched subsequently at a rate of $\cong 30$ K/s to room temperature. The HT-peak position and the dipole concentration of as grown and quenched crystals have been compiled in Table I.

At low La concentrations ($x=0.001$ and 0.005) the shift of the HT peak and the variation of the dipole concentration is not significant, whereas in the 1.5- and 3.3-mol %-doped crystals a shift up to 40 K can be observed

along with an increase of the dipole concentration. Quenching experiments performed on La-doped BaF_2 by Laredo *et al.*¹⁸ and Figueroa *et al.*,¹⁷ and La-doped SrF_2 by Suarez *et al.*¹⁹ and Figueroa *et al.*,¹⁷ also shows a shift of the HT-peak position towards lower temperatures. These authors have attributed this shift to an increase of the dislocation density in the crystals upon quenching. Because we are not convinced that dislocations in the crystals must be held responsible for the presence of the HT peak, as will be discussed later, we propose another explanation for the observed shift and the increase of the dipole concentration. It is noted that because of the similarities between La-doped SrF_2 and Ce-doped SrF_2 this explanation also applies to Ce-doped SrF_2 .

Although we assume in this paper that the Ce (or La) ions are distributed randomly over the SrF_2 lattice, interactions between the defects, especially if the distances between the ions are rather small, cannot be ignored;⁴ a deviation from the purely random distribution will then occur. The appearance of the 193 K peak and the discrepancy between the measured dipole concentration and the expected concentration on basis of Eq. (7) may be a consequence of this deviation. The defect structure is determined by the temperature at which the mobility of the rare-earth ions becomes so small that the rare-earth position can be considered as “frozen” in the fluorite lattice. Quenching the crystals from a temperature at which the rare-earth ions are mobile will then result in a defect structure different from the defect structure in the as grown crystals. As a consequence the ionic conductivity and the concentration of isolated dipolar complexes changes, which may account for the observed shift of the HT peak and the increased dipole concentration in the 1.5- and 3.3-mol % La-doped crystals. In the 0.1- and 0.5-mol %-doped crystals each La ion is isolated from other La ions so quenching does not change the defect structure and the HT peak remains at a fixed position.

D. The HT peak

From the results discussed until now we have arrived at conclusions concerning the defect structure which will be essential in the discussion of the HT peak. The defect structure depends upon the Ce concentration, and based on our observations we can distinguish between three characteristic concentration regions.

(i) In the dilute region, $x < 0.005$, the Ce ions are involved in an NN dipole complex, distributed randomly over the SrF_2 lattice. The average spacing between the defects is relatively large and the dipoles can be considered

TABLE I. HT-peak position (T_m) and dipole concentration (N_d) of as-grown and quenched crystals of $\text{Sr}_{1-x}\text{La}_x\text{F}_{2+x}$.

x	T_m (K)	As grown		Quenched	
		T_m (K)	N_d (10^{25} m^{-3})	T_m (K)	N_d (10^{25} m^{-3})
0.001	375	374	2.5 ± 0.3	374	2.4 ± 0.3
0.005	365	363	5.9 ± 0.3	363	6.3 ± 0.3
0.015	337	325	7.0 ± 0.3	325	12.0 ± 0.3
0.033	301	257	2.8 ± 0.3	257	4.6 ± 0.3

to be isolated from other defects.

(ii) For concentrations between 0.5 and 10 mol %, the intermediate concentration region, the defect structure is much more complicated. At 1 mol % the NN dipoles begin to interact significantly, leading to a decrease of the orientational polarization of $\text{Ce}^{3+}\text{-F}^-$ dipoles, and consequently the intensity of the dipolar relaxation peak decreases. The HT peak shifts towards lower temperatures due to an increased ionic conductivity.

(iii) For concentrations higher than $x = 0.1$, the concentrated region, the HT peak stops shifting and the width is rather small (Fig. 2). Dipoles are not observed anymore.

Crucial in the discussion of the results to be presented further in this paper is the interpretation of the HT peak. In Ref. 1 we showed that the HT peak must be associated with ionic conductivity leading to charge accumulation at the crystal surfaces. Recently, however, Laredo *et al.* have questioned our conclusions. They state that the HT peak, observed in ITC recordings of rare-earth doped SrF_2 and BaF_2 , is caused by the relaxation of charged ions associated with dislocations present in the crystals.^{5,17-21} Instead a peak located at higher temperatures than the HT peak, the so-called *E* peak, has been attributed to accumulation of charges at the crystal surfaces by Laredo *et al.* We stress that we have never observed an *E* peak in our ITC recordings. We think, therefore, that the origin of this peak must not be sought in the studied crystals. Instead electron injection across the electrode-crystal interface might be responsible for the *E* peak. In our ITC experiments this injection is not possible due to the Teflon® insulation layers between the electrodes and the crystal.

Our experimental ITC setup and the interpretation of the HT peak are in many respects equivalent to the setup and the interpretation employed by Kessler *et al.*²² to investigate CdF_2 doped with NaF. These authors also observe a dipole relaxation peak along with a high-temperature peak. The HT peak is dealt with in the same way as expressed by Eq. (6).

1. The HT peak in the dilute concentration region

In this concentration region we will employ a model in which interstitial F^- ions, dissociated from $\text{Ce}^{3+}\text{-F}^-$ dipolar complexes, migrate through the lattice by jumping from one interstitial site towards another interstitial site. This jump process of F^- ions leads to ionic conductivity if a polarizing electric field is present. As a result accumulation of F^- ions at the positive electrode occurs. The relaxation of these accumulated F^- ions in an ITC experiment leads to a depolarization current which is observed as the HT peak in the ITC recordings.

The ionic conductivity due to the hopping of F^- ions in a cubic lattice can be described by

$$\sigma(T) = n \frac{q^2 s^2}{6k_B T} \Gamma \quad (9)$$

(Ref. 23), where n is the concentration of dissociated F^- ions, q is the F^- charge, s is the jump distance, and Γ is the number of F^- jumps per second which is activated thermally,

$$\Gamma = \Gamma_0 \exp \left[\frac{-E_a}{k_B T} \right]. \quad (10)$$

Γ_0 is a proportionality constant and E_a is the activation energy, which is determined by the potential barrier height experienced by a jumping F^- ion. Equation (9) is valid only if the fluorite lattice is not disturbed by defects, therefore, the Ce concentration must be low.

From statistical mechanics one can derive that the concentration n of dissociated F^- ions as a function of the Ce concentration is equal to

$$n = N \left[\frac{x(1-gx)}{g} \right]^{1/2} \exp \left[\frac{-E_d}{2k_B T} \right], \quad (11)$$

where $N = 2.05 \times 10^{28} \text{ m}^{-3}$, which is the concentration of interstitial sites in SrF_2 , E_d is the dissociation energy of a $\text{Ce}^{3+}\text{-F}^-$ dipolar complex, g is the number of bound interstitial F^- sites surrounding a Ce^{3+} ion. Equation (11) is valid only if the bound positions surrounding one particular Ce ion do not overlap with bound positions surrounding another Ce ion, therefore, the condition $gx \ll 1$ should be fulfilled.

Combining (9) and (11) gives the well-known Arrhenius equation for ionic conductivity

$$\sigma(T) = \frac{\sigma_0}{T} \exp \left[\frac{-(E_a + \frac{1}{2}E_d)}{k_B T} \right], \quad (12)$$

where σ_0 is proportional to \sqrt{x} . From (4) and (12) we derive for the shift of the HT peak with the Ce concentration

$$\frac{dT}{d(\log_{10}x)} = \frac{-\ln 10}{2} \left[\frac{1}{T_m} + \frac{E_a + \frac{1}{2}E_d}{k_B T_m^2} \right]^{-1}, \quad (13)$$

in which T_m is the position of the maximum of the HT peak [Fig. 2(a)]. Equation (13) does not depend upon the ITC sample-cell configuration. Inserting a value of 1.34 eV for $E_a + \frac{1}{2}E_d$ in Eq. (13), as has been obtained in Ref. 6. and with T_m approximately 370 K, we calculate a HT-peak shift of -10 K/decade. This is indeed what can be observed in the concentration region up to $x = 0.005$ [Fig. 2(a)]. Also SrF_2 doped with rare-earth ions other than Ce shows this shift in the dilute concentration region (Ref. 1 and references therein).

From Eq. (4) and Eq. (12) an expression relating the HT-peak position and the activation energy $E_a + \frac{1}{2}E_d$ can be derived,

$$\frac{-1}{T_m} + \frac{E_a + \frac{1}{2}E_d}{k_B T_m^2} = \frac{\sigma_0}{T_m} \exp \left[\frac{-(E_a + \frac{1}{2}E_d)}{k_B T_m} \right] \frac{f}{b \epsilon_0 \epsilon_s}. \quad (14)$$

If the term $1/T_m$ is neglected and the doping concentration is kept constant, the HT-peak position is proportional to $E_a + \frac{1}{2}E_d$. The proportionality constant is determined by σ_0 and the sample-cell configuration.

In the last few years we have performed ITC experiments on SrF_2 doped with La, Ce, Pr, Nd, Eu, Sm, Gd, Dy, Er, Yb, Lu, and Y (Ref. 1 and references therein) and

BaF₂ doped with La,²⁴ Gd,¹⁵ Eu, and Yb. All experiments were performed with the same experimental parameters such as crystal dimensions, ITC sample-cell configuration, etc. In Fig. 4 the position of the HT peak for one particular doping concentration ($x = 0.001$) in the dilute concentration region has been plotted. The position depends on both the dopant and the host crystal. The variation of the HT-peak position as a function of rare-earth dopant must be attributed to changes in the dissociation energies of R^{3+} -F⁻ dipolar complexes (NN as well as NNN), whereas the shift of the HT peak towards lower temperatures in going from SrF₂ to BaF₂ is attributed to a change in both E_a and E_d .

In the accompanying paper⁶ a value of 1.34 ± 0.02 eV for the activation energy of the ionic conductivity in dilutely Ce-doped SrF₃ crystals has been obtained. Employing this value and the observed HT-peak position of 0.1-mol % Ce-doped SrF₂ (370 K), the proportionality constant between $(E_a + \frac{1}{2}E_d)$ and T_m has been obtained. It is not expected that this constant varies significantly in going from SrF₂ to BaF₂ or if other dopant ions than Ce are used. The activation energies $E_a + \frac{1}{2}E_d$ can now be calculated straightforwardly from the HT-peak positions. If we use for E_a of SrF₂ a value of 0.945 eV, as has been reported by Bollmann *et al.*²⁵ and by Schoonman *et al.*,²⁶ and a value of 0.79 eV for BaF₂ obtained by Bollmann²⁷ the dissociation energy of the dipolar complexes can be obtained; the results have been compiled in Table II. The stochastic error in E_d is approximately 0.03 eV; however, there may also be some systematic error due to uncertainties in the proportionality constant between $(E_a + \frac{1}{2}E_d)$ and T_m . This error is estimated to be 0.05 eV.

If rare-earth-doped SrF₂ is considered, the association energy of R^{3+} -F⁻ dipolar complexes decreases in going from La to Er and slightly increases for the ions with still smaller radii (Yb and Lu). The dipolar complexes in BaF₂ show an increase in association energy as the ionic radius of the rare-earth ion decreases. If the results are compared with theoretically calculated association energies (Corish *et al.*³), which have been compiled in the fifth column of Table II, the same trends, although less pronounced, can be observed as a function of the rare-earth ionic radius. The absolute values, however, may deviate

appreciably from the calculated values. Association energies calculated by Wapenaar *et al.*,²⁸ with semiempirical lattice potentials, have also been included in Table II. These results show a better agreement with our experimental results. Corish *et al.* have calculated for Y^{3+} -F⁻ dipolar complexes in SrF₂ an anomalous stability; we, on the contrary, find an anomalous instability as compared to the rare-earth ions. Bollmann *et al.*²⁵ have also reported a rather small association energy of Y^{3+} -F⁻ complexes in SrF₂ (0.16 eV). The fact that Y^{3+} is not a member of the series of lanthanide ions, and, therefore, has different chemical characteristics is probably responsible for this low association energy.

Summarizing, we arrive at the following conclusions about ionic conductivity in the dilute region.

(i) The ionic conductivity for Ce concentrations below $x = 0.005$ can be described by the Arrhenius expression.

(ii) The shift of the HT peak with the concentration agrees with this conductivity model.

(iii) The shift of the HT peak as a function of the dopant ion and the host material can be explained by a change in E_a and E_d .

(iv) The absolute values of theoretically determined dissociation energies of R^{3+} -F⁻ dipolar complexes may deviate considerably from experimentally obtained values, although the trends with rare-earth ionic radius compare quite well.

2. The HT peak in the intermediate and concentrated region

At Ce concentrations higher than 0.5 mol % the shift of the HT peak with the Ce concentration is much more than -10 K/decade; furthermore, the width of the HT peak [Fig. 2(b)] increases. These features cannot be described with an Arrhenius-type ionic conductivity. Instead, new conductivity models should be applied in this concentration region. In order to demonstrate the deviations from Arrhenius-type ionic conductivity, we have performed ITC experiments on partially polarized (La-doped SrF₂) crystals.

Usually an ITC experiment is performed by polarizing the crystal at a temperature higher than T_m of the HT peak. The mobility of the interstitial F⁻ ions is then large enough to fully polarize the crystal. If, however, the polarization temperature is chosen below T_m and if the polarization time is not sufficiently long, the crystal is partially polarized. In Fig. 5 the HT-peak position as a function of the polarization fraction (α), defined as the fraction of maximal polarization, can be seen. In the dilute concentration region ($x = 0.001$) the peak remains almost at a fixed position, for intermediate concentrations a shift towards lower temperatures is observed as the polarization fraction decreases. The heavily doped crystal ($x = 0.3$) also shows a shift towards lower temperatures. This shift is, however, less pronounced than for intermediate concentrations.

If the ionic conductivity can be described by the Arrhenius equation, we do not expect that the dielectric constant of Ce-doped SrF₂ changes significantly with the temperature. Equation (4) can now be used to describe the

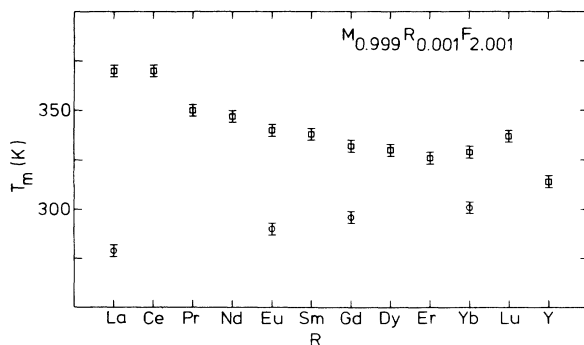


FIG. 4. The position of the HT peak of 0.1-mol % RF_3 -doped MF_2 crystal. R^{3+} is a member of the lanthanide series or Y^{3+} . □, MF_2 is SrF₂; ○, MF_2 is BaF₂.

TABLE II. Compilation of the activation energies ($E_a + \frac{1}{2}E_d$) for Arrhenius-type ionic conductivity and the dissociation energies (E_d) of $R^{3+}\text{-F}^-$ dipolar complexes of MF_2 ($M = \text{Sr}$ or Ba) single crystals doped with 0.1 mol % trivalent cation impurities (R) as has been obtained from ITC recordings. In addition, theoretically calculated values for E_d by Corish *et al.* (Ref. 3) and Wapenaar *et al.* (Ref. 28) have been compiled.

System $\text{MF}_2\text{:}R$	Dipole type	$E_a + \frac{1}{2}E_d$ (eV)	E_d (eV)	E_d (eV) Ref. 3	E_d (eV) Ref. 28
SrF ₂ :La	NN	1.34	0.79	0.592	0.75
SrF ₂ :Ce	NN	1.34	0.79		
SrF ₂ :Pr	NN	1.27	0.65		
SrF ₂ :Nd	NN	1.26	0.62		
SrF ₂ :Eu	NN	1.23	0.57	0.563	0.58
SrF ₂ :Sm	NN	1.22	0.56		
SrF ₂ :Gd	NN	1.20	0.51	0.529	
SrF ₂ :Gd	NNN			0.535	
SrF ₂ :Dy	NNN	1.20	0.51		
SrF ₂ :Er	NNN	1.18	0.47	0.534	
SrF ₂ :Yb	NNN	1.19	0.49	0.543	
SrF ₂ :Lu	NNN	1.22	0.55	0.537	0.55
SrF ₂ :Y	NNN	1.14	0.38	0.592	
BaF ₂ :La	NNN	1.01	0.44	0.546	0.39
BaF ₂ :Eu	NNN	1.05	0.52	0.555	0.45
BaF ₂ :Gd	NNN	1.07	0.56	0.568	
BaF ₂ :Yb	NNN	1.09	0.60	0.572	

ionic thermocurrent. The only change upon partial polarization of the crystal is the substitution of αP_0 for P_0 in Eq. (4). The HT peak obtained after partial polarization must, therefore, be identical in shape and position to the fully polarized case; this agrees with the results obtained for the dilutely doped crystal in Fig. 5.

In order to understand the behavior of the HT peak with the Ce concentration (Fig. 2) and the polarization fraction (Fig. 5), the defect structure should be considered. At concentrations above $x = 0.005$, NN and NNN sites of

a particular Ce^{3+} ion start to overlap with NN or NNN sites of other Ce^{3+} ions; Eq. (9) as well Eq. (11), and consequently the Arrhenius equation, Eq. (12), will no longer be valid. In recent papers¹⁰⁻¹³ a model has been proposed to explain the shift of the HT peak between $x = 0.005$ and 0.1. The overlap of NN and NNN sites leads, in this model, to easily conducting areas in the lattice. It is assumed that F^- ions can hop relatively easily from one Ce^{3+} ion to another Ce^{3+} ion without the need to dissociate from a Ce^{3+} ion and without the need to overcome the high potential energy barriers present in pure SrF_2 . The mobility of an interstitial F^- ion increases drastically, leading to ionic conductivities higher than expected with Eq. (12). Although it is not expected that the potential energy barriers for F^- jumps in the vicinity of Ce, impurities remain the same if additional impurities are nearby (see also the discussion of the NN relaxation peak), the main idea is that the potential energy barriers close to a Ce ion are low ($\cong 0.6$ eV) as compared to the barriers in pure SrF_2 ($\cong 1.0$ eV). We are now dealing with the phenomenon of hopping ionic conductivity in a random medium. We have given in Fig. 6 an one dimensional illustration of F^- ions in a random potential energy barrier

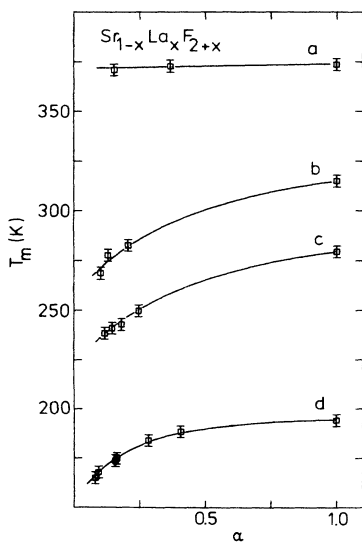


FIG. 5. The position of the HT peak of $\text{Sr}_{1-x}\text{La}_x\text{F}_{2+x}$ plotted vs the fraction of maximal polarization. (a) $x = 0.001$; (b) $x = 0.03$; (c) $x = 0.057$; (d) $x = 0.30$.

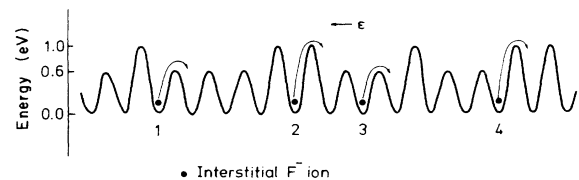


FIG. 6. An illustration of hopping ionic conductivity in an one-dimensional random medium. ϵ represents the applied electric field.

structure. A valley in this figure corresponds with a possible interstitial F^- site, and the saddle points represent the barriers for F^- jumps. F^- ions are placed at the numbered positions. If a polarizing electric field is applied, the F^- ions will respond to this field by hopping from one interstitial site to an adjacent site. The ions located at positions 1 and 3 will, on the average, jump sooner to the right than the ions at positions 2 and 4 because the latter ones see a larger barrier on the right. The mobile ions (1 and 3) jump until a high potential barrier is encountered: Then it takes a while before a next jump is made. After some time a steady-state current is built up leading to dc ionic conductivity.

If a crystal with a random potential barrier structure due to a high doping level, is partially polarized, only the most mobile F^- ions contribute to this polarization. During depolarization in an ITC experiment these mobile ions will relax at relatively low temperatures, which accounts

for the observed shift of the HT peak in Fig. 5. The mobile F^- ions are also responsible for the broadening of the HT peak observed in Fig. 2(b). Furthermore, as the Ce concentration increases the relative abundance of low potential energy barriers increases; the F^- ions percolating through the lattice by hopping over these low energy barriers are responsible for an increased ionic conductivity and accordingly the HT-peak shifts towards lower temperatures.

With the model of hopping ionic conductivity in a random potential energy barrier structure we have been able to explain qualitatively the phenomena associated with the HT peak; i.e., the shift of the HT peak with the Ce concentration, the increase of the width of the HT peak, and the shift of the HT peak upon partial polarization of the crystals. In the accompanying paper,⁶ in which impedance measurements are presented, we will provide quantitative data in support of the above-described model.

-
- ¹P. Dorenbos and H. W. den Hartog, *Phys. Rev. B* **31**, 3932 (1985).
- ²C. G. Andeen, J. J. Fontanella, M. C. Wintersgill, P. J. Welchers, R. J. Kimble, Jr., and C. E. Matthews, Jr., *J. Phys. C* **14**, 3557 (1981).
- ³J. Corish, C. R. A. Catlow, P. W. M. Jacobs, and S. H. Ong, *Phys. Rev. B* **25**, 6425 (1982).
- ⁴P. J. Bendall, C. R. A. Catlow, J. Corish, and P. W. M. Jacobs, *J. Solid State Chem.* **51**, 159 (1984).
- ⁵E. Laredo, N. Suarez, A. Bello, M. Puma, D. Figueroa, and J. Schooman, *Phys. Rev. B* **32**, 8325 (1985).
- ⁶P. Dorenbos, H. W. den Hartog, R. Kruizinga, and S. Vrind, following paper, *Phys. Rev. B* **35**, 5774 (1987).
- ⁷B. P. M. Lenting, J. A. J. Numan, E. J. Bijvank, and H. W. den Hartog, *Phys. Rev. B* **14**, 1811 (1976).
- ⁸P. Müller, *Phys. Status Solidi A* **67**, 11 (1981).
- ⁹J. Fontanella, D. L. Jones, and C. Andeen, *Phys. Rev. B* **18**, 4454 (1978).
- ¹⁰H. W. den Hartog and J. C. Langevoort, *Phys. Rev. B* **24**, 3547 (1981).
- ¹¹J. Meuldijk and H. W. den Hartog, *Phys. Rev. B* **28**, 1036 (1983).
- ¹²J. Meuldijk, R. v.d. Meulen, and H. W. den Hartog, *Phys. Rev. B* **29**, 3153 (1984).
- ¹³J. Meuldijk, H. H. Mulder, and H. W. den Hartog, *Phys. Rev. B* **25**, 5204 (1982).
- ¹⁴A. B. Aalbers and H. W. den Hartog, *Phys. Rev. B* **19**, 2163 (1979).
- ¹⁵H. W. den Hartog, P. Dorenbos, and W. Postma, *Phys. Rev. B* **34**, 7496 (1986).
- ¹⁶C. Andeen, J. Fontanella, and D. Schuele, *J. Appl. Phys.* **43**, 2216 (1971).
- ¹⁷D. Figueroa, E. Laredo, M. Puma, and N. Suarez, *Cryst. Lattice Defects*, **9**, 167 (1982).
- ¹⁸E. Laredo, M. Puma, and D. R. Figueroa, *Phys. Rev. B* **19**, 2224 (1979).
- ¹⁹N. Suarez, E. Laredo, D. Figueroa, and M. Puma. *Radiat. Eff.* **75**, 105 (1983).
- ²⁰E. Laredo, M. Puma, N. Suarez, and D. Figueroa, *Solid State Ionics* **9&10**, 497 (1983).
- ²¹M. Puma, A. Bello, N. Suarez, and E. Laredo, *Phys. Rev. B* **32**, 5424 (1985).
- ²²A. Kessler and W. Appel. *Radiat. Eff.* **75**, 85 (1983).
- ²³W. Hayes, *Crystals With the Fluorite Structure* (Oxford University Press, London, 1974).
- ²⁴H. W. den Hartog, K. F. Pen, and J. Meuldijk, *Phys. Rev. B* **28**, 6031 (1983).
- ²⁵W. Bollmann, P. Görlich, E. Hauk, and H. Mothes, *Phys. Status Solidi A* **2**, 157 (1970).
- ²⁶J. Schooman and H. W. den Hartog, *Solid State Ionics* **7**, 9 (1982).
- ²⁷W. Bollmann, *Cryst. Res. Technol.* **16**, 1039 (1981).
- ²⁸K. E. D. Wapenaar and C. R. A. Catlow, *Solid State Ionics* **2**, 245 (1981).